European Review for Medical and Pharmacological Sciences 2021; 25: 116-126

Integrative analysis of the characteristics of lipid metabolism-related genes as prognostic prediction markers for hepatocellular carcinoma

P. ZHU[1], F.-F. LI[2], J. ZENG[4], D.-G. TANG[3], W.-B. CHEN[3], C.-C. GUO[1]

[1]Central Lab of Shenzhen Pingshan People's Hospital, Shenzhen, China
[2]The First Class Ward 2 of The First Affiliated Hospital of Jinan University, Guangzhou, China
[3]Department of Clinical Medical Research Center, The Second Clinical Medical College of Jinan University, The First Affiliated Hospital Southern University of Science and Technology, Shenzhen People's Hospital, Shenzhen, China
[4]The Centre of Medical Genetics and Molecular Diagnosis, University of Chinese Academy of Sciences-Shenzhen Hospital, Shenzhen, China

Peng Zhu and FeiFei Li contributed equally to this work

Abstract. – OBJECTIVE: Dysregulated lipid metabolism has been reported in the progression of hepatocellular carcinoma (HCC). In the present study, we investigated the molecular characteristics of lipid-metabolism-related genes (IMRGs) as prognostic markers for HCC.

MATERIALS AND METHODS: Multi-dimensional bioinformatics analyses were performed to comprehensively analyze IMRGs, and to construct prognostic prediction signatures.

RESULTS: Data of 770 HCC patients and their corresponding 776 IMRGs were downloaded from three databases. Patients were classified into 2 molecular clusters that were associated with overall survival, clinical characteristics, and immune cells. The biological functions of the IMRGs differentially expressed between the 2 clusters were associated with tumor-related metabolic pathways. A 6 IMRG signature (6-IS), consisting of *FMO3*, *SLC11A1*, *RNF10*, *KCNH2*, *ME1*, and *ZIC2*, was established as an independent prognostic factor for HCC. The performance of the signature of 6-IS prognostic was verified in a validation set and compared to an external data set. It was revealed that the 6-IS could effectively predict the prognosis of patients with HCC.

CONCLUSIONS: This study provides new insights into the role of IMRGs in the pathogenesis of HCC, and presents a novel signature (6-IS) to predict the prognosis of HCC.

Key Words:
Lipid metabolism, Gene, Prognosis, Hepatocellular carcinoma, Bioinformatics analysis.

Introduction

Hepatocellular carcinoma (HCC) is a common malignant tumor that is characterized by high metastatic potential and poor prognosis[1]. Most HCC diagnoses are made when the disease is in the advanced stages. In these stages, patients do not effectively benefit from surgery or chemoradiotherapy[2]. Recently, therapies based on biological targets have been proposed for HCC patients[3]. However, the clinical benefits of the available biomarkers for early diagnosis and prognostic assessment of HCC remain limited. Therefore, it is important to study the pathogenesis of HCC and identify specific targets that can be used to improve both diagnosis and prognostic predictions.

Many metabolic functions in humans occur in liver cells[4]. As a consequence of an important site for lipid metabolism, HCC results in many lipid metabolic abnormalities[5], such as increased *de novo* synthesis of fatty acids, suppressed oxidation levels, high secretion of insulin and insulin-like growth factors, and abnormal metabolism of phosphatidylcholine[6]. These metabolic processes provide intermediate energy substrates that enable HCC cells to grow, proliferate, and metastasize[7]. In addition, several enzymes and signaling molecules, such as 3-hydroxy-3-methylglutaryl-coenzyme A reductase, and the AKT/mTORC1 pathway regulate lipid metabolism in HCC cells. These

Corresponding Authors: Wenbiao Chen, MD; e-mail: chanwenbiao@sina.com
Changchun Guo, MD; e-mail: guoccpsh@163.com

metabolic enzymes and pathways can be used as biomarkers for the diagnosis and treatment of HCC[8].

Studies have determined biological phenotypes and molecular classifications of HCC on the basis of lipid metabolic patterns[9]. For example, the *de novo* fatty acid synthesis phenotype in tumor cells has been associated with the upregulation of lipid-related genes at multiple levels, e.g., at transcription, translation, post-translational modification, and enzyme activity, as well as the influence of these genes on oncogenes [10]. The molecular classification of HCC based on lipid metabolism-related genes revealed distinct tumor subtypes. By utilizing bioinformatics, Bidkhori et al[11] grouped patients with HCC into three clusters with distinct metabolic and signaling pathways at the genomic, transcriptomic, and proteomic levels. These clusters were associated with clinical features and survival rates. However, lipid metabolic pathways and molecules have not been fully exploited for the prognostic prediction of HCC.

In this study, data of 770 HCC patients were grouped into two molecular clusters based on 776 IMRGs. The two molecular clusters were associated with clinical features, immune infiltration, and tumor metabolism-related biological processes. We also established a prognostic signature for the HCC patients. A flow chart showing the protocol used in this study is shown in **Supple-mentary Figure 1**. This study elucidated the molecular bases of lipid metabolism involved in the pathogenesis of HCC and highlights the lipid metabolism-related genes that could be utilized as prognostic markers for HCC.

Materials and Methods

Patient Characteristics and Genome Expression Datasets

Multiple datasets were obtained from several databases, including The Cancer Genome Atlas (TCGA), Gene Expression Omnibus (GEO), and the Database of Hepatocellular Carcinoma Ex-pression Atlas (HCCDB). A total of 371 samples obtained from TCGA were subjected to quality control and filtering processes. The 342 sam-ples that met these conditions were randomly distributed into training and validation sets. To avoid random allocation bias that could affect the stability of subsequent modeling, sampling was performed 100 times in advance to ensure that the training and validation sets exhibited consistent clinical features. The GSE15654 dataset was obtained from the GEO database. It was pre-processed for quality control and filtering, after which a total of 216 samples met the set conditions. The HCCDB18 dataset containing 212 samples and their corresponding clinical information was directly downloaded from the HCCDB database. Detailed information on the three datasets is presented in **Supplementary Table I**.

Molecular Classification of HCC Based on Lipid Metabolism-Related Genes

IMRGs were obtained from 6 lipid metabolism-related pathways (**Supplementary Table II**) from the Molecular Signature Database v7.0 (www.gsea-msigdb.org/gsea/msigdb). A total of 776 IMRGs were retained after the exclusion of overlapping genes. These 776 IMRGs were then extracted from the TCGA expression profile data, retaining only those genes with an expression value >0 in more than half of the samples. The 739 IMRGs that remained were used for subsequent analysis. The coxph R package was used to perform univariate Cox analysis on 739 IMRGs to extract HCC-related IMRGs. The HCC-related IMRGs were then processed using the non-negative matrix factorization (NMF) clustering algorithm of the NMF R package. The NMF analysis and 50 iterations were performed with the standard "brunet" pattern[12]. k values, indicating the optimal number of clusters, ranged from 2 to 10. The average contour width of the common member matrix was determined using the NMF R package, with the minimum member of each subclass set at 10. The optimal k value was determined from the indicators of "cophenetic", residual sum of squares (RSS), and silhouette. Differences in clinical features between the clusters separated by HCC-related IMRGs were compared using the Chi-square test. The Tumor Immune Estimation Resource (TIMER) (https://cistrome.shinyapps.io/timer/) algorithm was used to investigate associations between clusters and immune scores.

Construction of a Prognostic Signature Based on IMRGs

Using the DESeq2 algorithm from the limma R package, differential expression of HCC-related IMRGs between clusters was analyzed. IMRGs with a false discovery rate <0.05 and an absolute value of log2 fold change >1 were considered significant. Using the survival R package coxph function, HCC-related IMRGs with significantly

different expressions were subjected to univariate Cox analysis to determine their association with the survival of HCC. The log rank $p<0.01$ was set as the threshold. To narrow the gene range and build a prognostic model with high accuracy, the LASSO method was used to reduce the dimensionality and select the HCC-related IMRGs with the most significant differences in expression. The 10-fold cross validation methods were used to select the optimal values of the penalty parameter lambda[13]. Multivariate Cox analysis was then performed on the genes obtained in the preceding steps. The lowest value of the Akaike information criterion (AIC) within the Cox proportional regression model was calculated to retain the most significant genes with which to construct an IMRG signature. A risk score based on the IMRG signature set was calculated as follows: risk score = expression gene 1 × βgene 1 + expression gene 2 × βgene 2 + ⋯ + expression gene x × βgene x, where x was the number of IMRGs, and β was the coefficient value for each IMRG. The risk score was normalized to a z-score using the binormalization process algorithm. Samples with z-score values >0 and <0 were classified into high- and low-risk groups, respectively.

Statistical Analysis

The pheatmap R package was used to display the unsupervised hierarchical clustering heatmap of HCC-related IMRGs, while a volcano plot of the IMRGs differentially expressed between clusters was developed using the ggplot2 R package. Overall survival (OS) was estimated using the Kaplan-Meier (KM) method. The sensitivity and specificity of the survival curve were assessed using the receiver operating characteristic (ROC) curve by calculating the area under the curve (AUC) using the pROC R package. The gene ontology (GO) and Kyoto Encyclopedia of Genes and Genomes (KEGG) analyses were performed for the differentially expressed IMRGs using the clusterProfiler R package. The independent *t*-test and Mann-Whitney U test were performed to compare variables between groups (variables following normal and non-normal distributions, respectively). Associations between the IMRG signature and clinical features were analyzed by univariate and multivariate survival analyses. The associations between the IMRG signature and immune/stromal scores were determined by calculating the immune and stromal scores of each sample using the estimate R package and comparing high- and low-risk groups. The potential IMRG signature mechanisms were analyzed by Gene Set Enrichment Analysis (GSEA) using the GSVA R package. Pearson correlation coefficients were used to analyze the associations between the IMRG signature and biological functions. The prognostic value of the IMRG signature and other signatures were assessed using Harrell's concordance index (c-index) using the rms R package. The restricted mean survival time (RMST) is an index of the area under the KM curve at a specific time point. It was used to assess the predictive value of the IMRG signature at different time points. All statistical analyses were performed using SPSS v25.0 and R software version 3.4.0 (IBM Corp., Armonk, NY, USA). $p\leq0.05$ was considered statistically significant.

Results

Identification of Molecular Subtypes Based on IMRGs

Univariate Cox analysis was performed on 739 pre-processed IMRGs obtained from the TCGA dataset. A total of 324 HCC-related IMRGs were identified and used for HCC classification. The cophenetic coefficients, which indicate the stability of the classified cluster, were used to calculate the optimal k value. A comprehensive analysis was performed on the cophenetic, RSS, and silhouette indices. From this analysis, k=2 was selected as the optimal value. Consequently, 2 molecular subtypes (cluster 1 and cluster 2) were identified based on the IMRGs (**Supplementary Figure 2**). The matrix heat map exhibited clear boundaries based on the k value of 2, suggesting that the molecular subtype classification was stable (Figure 1A). The gene cluster heatmap of the 324 HCC-related IMRGs revealed marked differences between cluster 1 (C1) and cluster 2 (C2). The expression levels of HCC-related IMRGs in C2 were significantly higher than those in C1. In addition, there was a significant difference in the distribution of clinical features between C1 and C2 (Figure 1B). KM analysis revealed that C2 had a significantly shorter OS compared to C1 ($p=0.0099$) (Figure 1C). The accuracy of the molecular subtype classification based on the IMRGs was determined by comparing the associations between the 2 clusters and clinical features using the Chi-squared test. The pathological classifications of tumor (T) ($p=0.0002$), stage ($p=0.0478$), and grade ($p=0.0391$) were significantly different between the 2 clusters (**Supplementary Table III**). Immune score comparisons

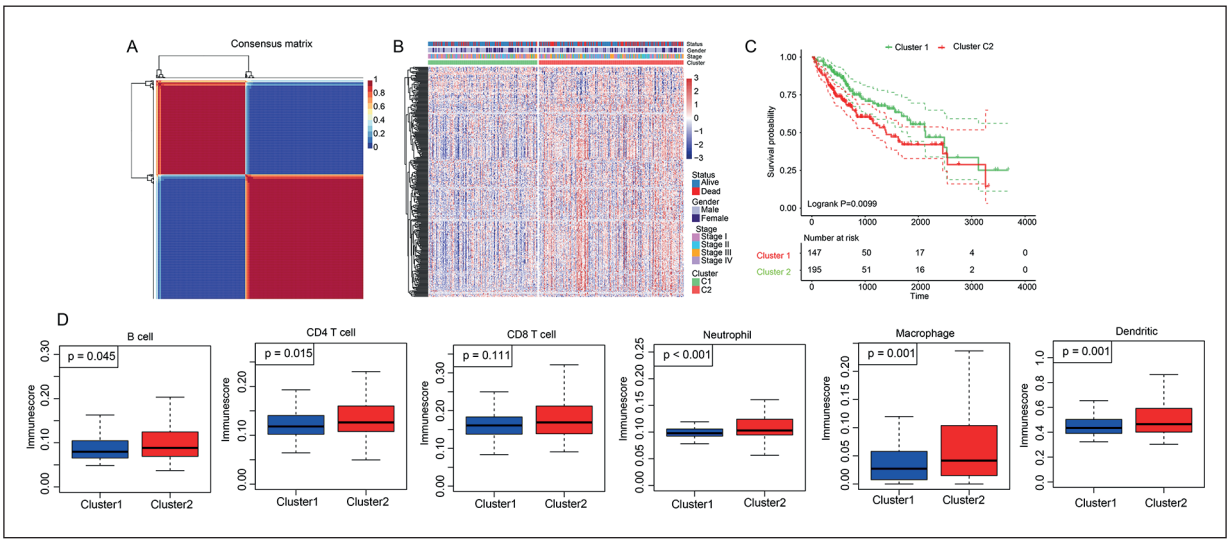

Figure 1. Classification of HCC based on IMRGs. **A,** Consensus map of NMF algorithm results for HCC patients, using k=2. **B,** Cluster heatmap of 324 prognosis-related IMRGs in the 2 HCC clusters. **C,** KM analysis of overall survival in the 2 HCC clusters. **D,** TIMER analysis of immune scores in the 2 clusters.

between the 2 clusters were performed using the TIMER algorithm. Except for CD8 cells, the immune scores of B cells (p=0.045), CD4 T cells (p=0.015), neutrophils (p<0.001), macrophages (p=0.001), and dendritic cells (p=0.001) were all significantly higher in cluster 2 than those in in cluster 1 (Figure 1D). These results revealed that the IMRG signature could classify HCC into distinct molecular subtypes and was associated with clinical characteristics.

Construction and Validation of an IMRG Signature

We first screened the IMRGs between clusters 1 and 2 and identified that a total of 400 IMRGs were significantly differentially expressed. Volcano and clustering maps revealed a distinct distribution of upregulated and downregulated IMRGs between the 2 clusters (**Supplementary Figure 3A, B**). GO analysis indicated that the differentially expressed IMRGs were primarily enriched in metabolic processes, such as glutamate and lactate metabolism, as well as in tumorigenesis-related processes such as cell-cell adhesion and cellular migration (**Supplementary Figure 3C**). In the KEGG analysis, IMRGs were predominantly enriched in metabolic pathways, such as glucagon signaling, metabolism of xenobiotics by cytochrome P450, and retinol metabolism (**Supplementary Figure 3D**). Functionally, the differentially expressed IMRGs were involved in tumorigenesis and metabolism-related pathways.

Univariate Cox regression and LASSO (Figure 2A, B) analyses were performed to select suitable genes from the 400 differentially expressed IMRGs; 20 significant genes were revealed by these two analyses. These were further subjected to a multivariate Cox regression analysis with the mimic AIC value = 466.72. Finally, we constructed the 6-IS (**Supplementary Table IV**) using the risk score formula. The associations between the 6 IMRGs and HCC survival were also evaluated. Unlike FMO3, which correlated with a good prognosis in high-risk groups, SLC11A1, RNF10, KCNH2, ME1, and ZIC2 correlated with shorter survival times in the high-risk group compared to those in the low-risk group (Figure 2C). Moreover, the 6-IS predicted significant differences in survival outcomes between C1 and C2. We then analyzed the expression profiles of the 6 IMRGs in the two clusters. Except for FMO3, the expression levels of other 5 IMRGs were all significantly higher in C2 than those in C1 (Figure 2D). Therefore, SLC11A1, RNF10, KCNH2, ME1, and ZIC2 were considered hazard indices, and FMO3 the protective index, for the construction of an independent prognostic IMRG signature.

According to the risk score calculations of the 6-IS in each sample, we depicted the risk score plot, survival status, and expression profiles of the 6 IMRGs in patients from the training set. We found that patients with HCC with high-risk scores exhibited higher mortality rates when compared to those with low-risk scores.

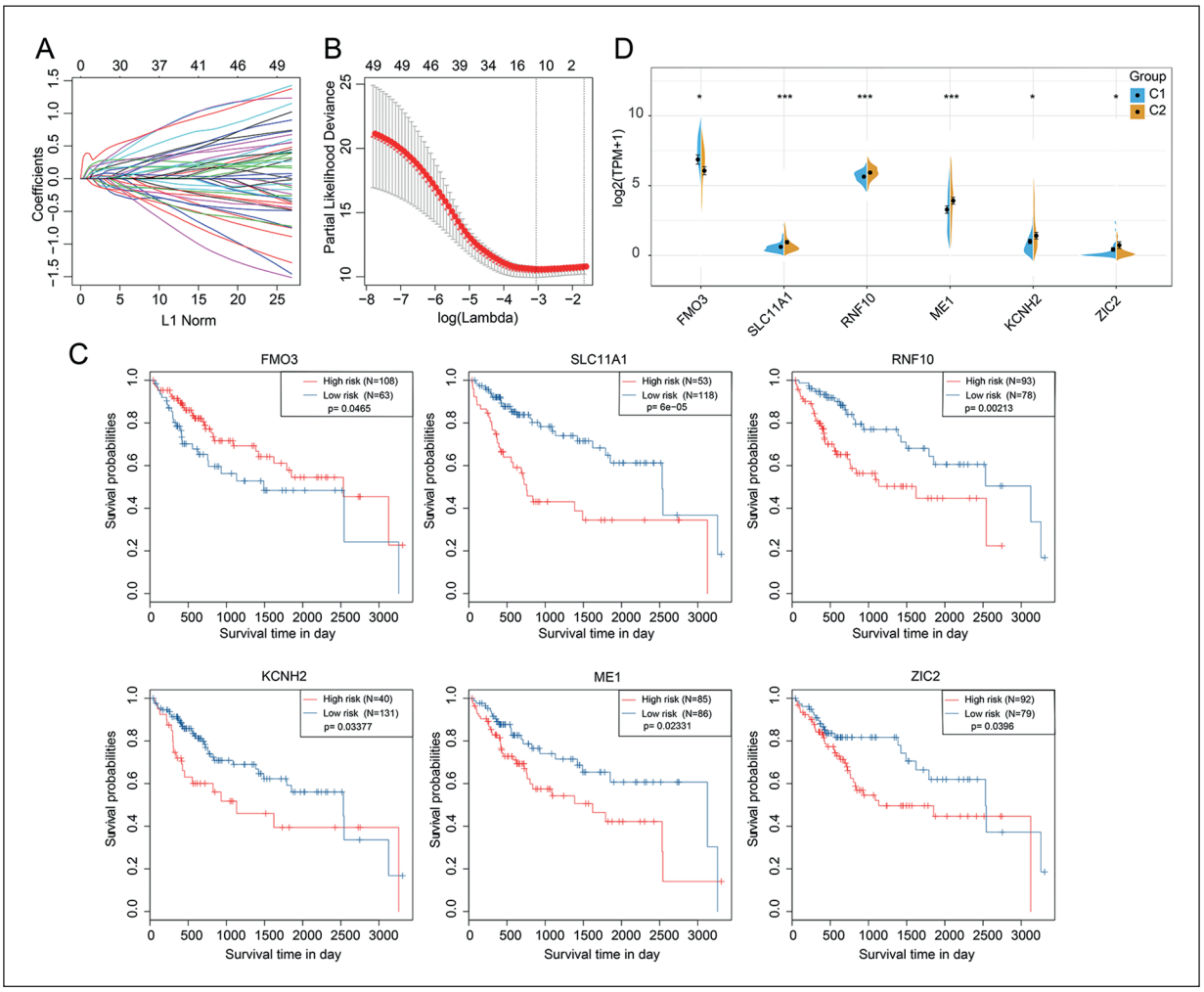

Figure 2. Selection of IMRGs for construction of a prognostic signature. **A,** LASSO analysis of IMRG coefficient profiles and the trajectory distribution of each independent IMRG. **B,** The confidence intervals under each lambda using 10-fold cross validation. **C,** KM analysis of the overall survival of HCC patients based on each of the 6 signature IMRGs. **D,** The expression of 6 IMRGs in the 2 clusters.

Changes in the expression of the 6 IMRGs with increased risk scores revealed that SLC11A1, RNF10, KCNH2, ME1, and ZIC2 were the hazard indices, while FMO3 was the protective index (Figure 3A). In the ROC analysis, the AUC for the 6-IS was 0.80, 0.82, and 0.84 for 1, 3, and 5 years, respectively, indicating a high prognostic prediction accuracy for the 6-IS (Figure 3B). In the training cohort, patients were divided into high- and low-risk groups. KM analysis based on 6-IS showed that the OS of the low-risk group was significantly higher than that of the high-risk group (Figure 3C). These results showed that the 6-IS could serve as an independent signature predicting the survival outcomes of patients with HCC in the validation (**Supplementary Figure 4A**), GSE15654 (**Supplementary Figure 4B**), and HCCDB18 sets (Supplementary Figure 4C). These findings show that the 6-IS could effectively predict the prognosis of patients with HCC.

Association of the 6-IS With Clinical Features and Molecular Characteristics of HCC

KM analysis showed that clinical features, including alpha-fetoprotein (AFP) (p= 0.02871), stage (p=3e−05), T (p=2e−05), N (lymph node) (p=0.02519), and M (metastasis) (p=0.00223) could be used to group the patients with HCC in the training set based on OS analysis (**Supplementary Figure 5**). We then predicted the OS

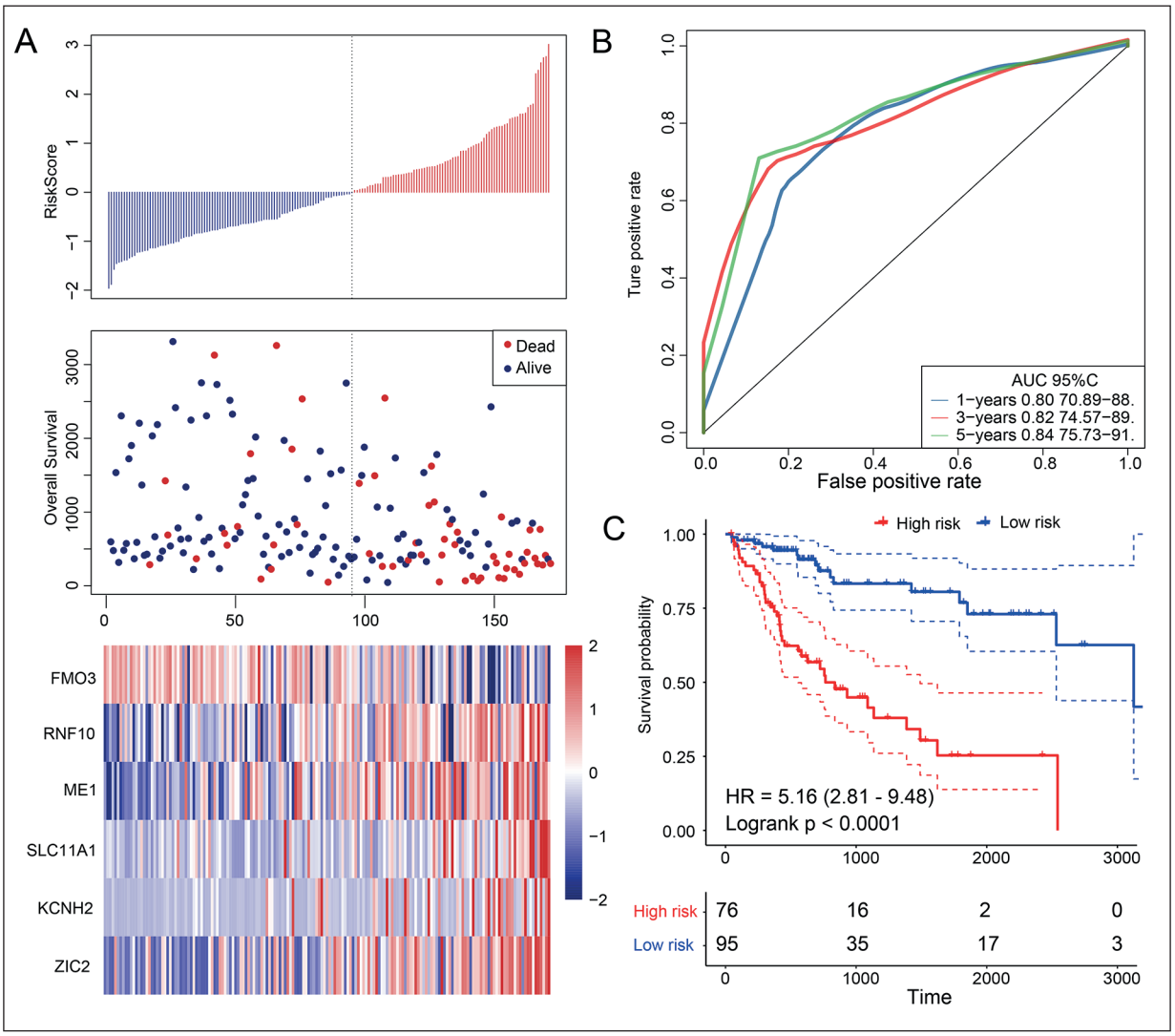

Figure 3. Prognostic prediction by 6-IS in the training set. **A,** Distributions of the risk scores, survival status, and expression of the 6 IMRGs, in patients with HCC. **B,** ROC curve analysis of the 6-IS for 1, 3, and 5 years. (C) KM analysis of overall survival of patients with HCC, based on 6-IS.

of patients with HCC using the 6-IS according to the above clinical features (AFP >20, AFP ≤20, T, N, M, Stage I+II, and Stage III+IV). It was found that the 6-IS could distinguish the low-risk group from the high-risk group. It was also revealed that patients with HCC in the high-risk group exhibited significantly shorter survival times than those in the low-risk group (Figure 4). Univariate and multivariate Cox analyses were performed to verify the prognostic value of 6-IS in patients with HCC from TCGA and HCCDB18 databases. It was concluded that 6-IS is an independent prognostic marker associated with survival when treated as a continuous variable in both TCGA (p=2.97E-09 and p=0.0049) and HCCDB18 (p=0.032 and p=0.0453) sets (Table I). We then calculated the immune, stromal, and estimate scores for each sample from TCGA. Both immune and estimate scores were significantly higher in the high-risk group than those in the low-risk group (**Supplementary Figure 6A**). Similar results were obtained for the HCCDB18 dataset (**Supplementary Figure 6B**). Using GSEA analysis, we compared the expression of IMRGs in samples from TCGA, HCCDB18, and GSE15654 sets. A single sample Gene Set Enrichment Analysis (ssGSEA) value was obtained and used to infer the associations between the 6-IS risk score and biological functions. Most of the biological functions, such as glyoxylate and

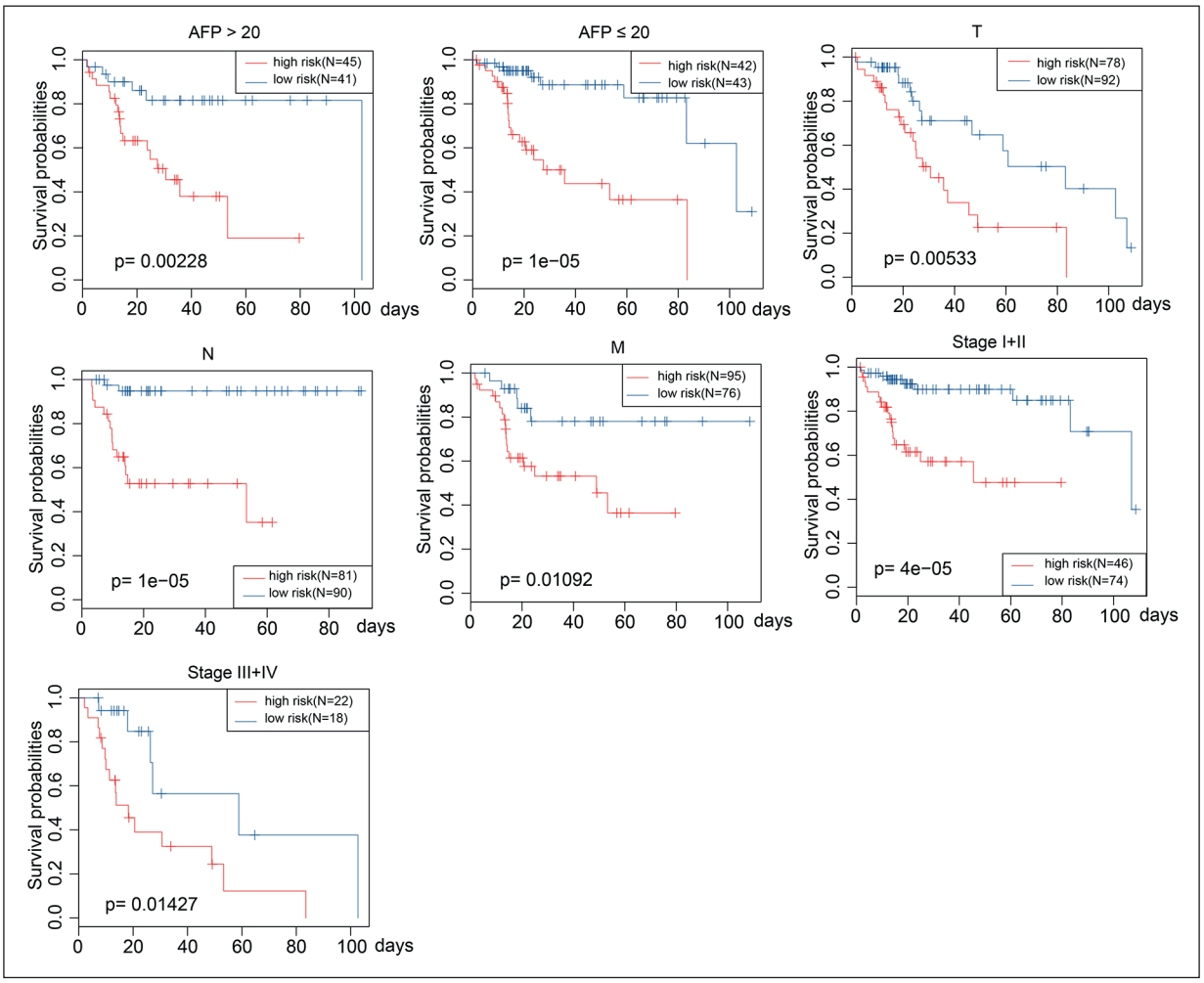

Figure 4. KM analysis of overall survival of HCC patients based on 6-IS, when patients were classified by clinical features (including AFP, TNM, and stage).

Table I. Univariate and multivariable Cox analyses to identify prognostic-related clinical factors.

Variables	Univariate analysis			Multivariable analysis		
	HR	95% CI of HR	*p*-value	HR	95% CI of HR	*p*-value
Entire TCGA cohort						
Risk score (High/Low)	3.025	2.099-4.361	2.97E-09	1.997	1.234-3.233	0.0049
Age	1.008	0.994-1.022	0.231	1.021	1.001-1.041	0.0434
Gender (Male/Female)	0.8	0.556-1.150	0.229	0.881	0.542-1.43	0.6072
AFP	1.748	1.105-2.765	0.017	2.455	1.392-4.333	0.0019
T3/T4 *vs.* T1/T2	2.838	1.981-4.067	1.32E-08	1.285	0.775-2.13	0.3318
N1/N2 *vs.* N0	1.617	1.112-2.349	0.012	1.030	0.554-1.916	0.9248
M1/MX *vs.* M0	1.795	1.235-2.608	0.002	2.972	1.611-5.482	0.0005
Stage III/IV *vs.* Stage I/II	2.767	1.893-4.046	1.51E-07	0.851	0.585-1.239	0.4010
G3/G4 *vs.* G1/G2	1.069	0.736-1.553	0.724	1.737	1.054-2.864	0.0304
ICGA cohort						
Risk score (High/Low)	2.088	1.066-4.089	0.032	1.955	0.989-3.859	0.0453
Age	1.015	0.979-1.052	0.406	1.004	0.968-1.041	0.8422
Gender (Male/Female)	0.516	0.256-1.039	0.064	0.360	0.166-0.782	0.0098
Stage III/IV *vs.* Stage I/II	2.737	1.415-5.295	0.0028	3.462	1.711-7.003	0.0006

dicarboxylate metabolism, drug metabolism by cytochrome p450, and beta-alanine metabolism, were negatively associated with 6-IS risk scores. In contrast, biological functions associated with tumorigenesis, including glycerophospholipid metabolism, fatty acid metabolism, cell cycle, and RNA degradation were positively correlated with 6-IS risk scores (**Supplementary Figure 7A**). The clustering heatmap based on ssGSEA values revealed the biological pathways positively or negatively correlated with the 6-IS risk scores (**Supplementary Figure 7B**).

Comparison of 6-IS With External Models

A six gene signature[14], an eight gene signature[15], a six gene-based prognostic signature[16], and a four gene signature[17], were used as the external data set for validation. These signatures were established to calculate the risk score and assess the OS of patients in TCGA using methods similar to those in our study. In line with 6-IS, KM analysis showed that all four models could assign patients with HCC into high- and low-risk groups. The high-risk groups exhibited significantly shorter survival times compared to low-risk groups (Figure 5A-D). However, except for the eight gene signature (0.813), which showed similar results to our study, ROC analysis revealed that the average AUC values at 1, 3, and 5 years from the six gene signature (0.613), six gene-based prognostic signature (0.770), and four gene signature (0.686) were low compared to 6-IS (0.82) (Figure 5A-D). In c-index analysis, 6-IS exhibited a better prognostic ability than the other four models (Figure 5E). RMST analysis also found that 6-IS performed better than the other four models in the prognostic prediction of HCC patients (Figure 5F). These results show 6-IS as a robust prognostic prediction signature.

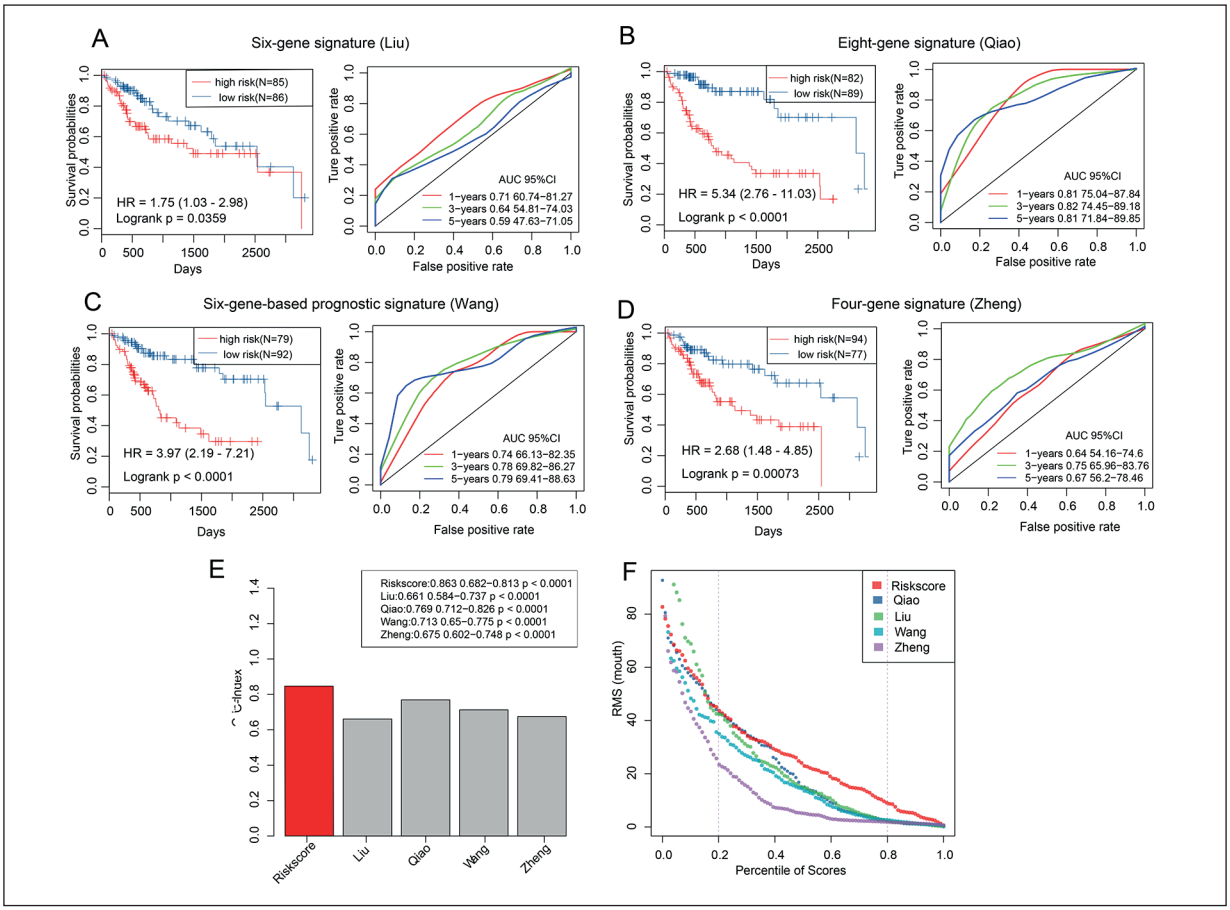

Figure 5. Comparison between 6-IS and external models. ROC curve analysis of the 6-IS for 1, 3, and 5 years, and KM analysis of overall survival in HCC patients according to the (**A**) six gene signature, (**B**) eight gene signature, (**C**) six gene-based prognostic signature, and (**D**) four gene signature. **E,** C-index analysis of 6-IS and four other external models. **F,** The RMST analysis of 6-IS and four other external models.

Discussion

Tumorigenesis is accompanied by metabolic reprogramming of various nutrients that sustain cancer cell survival, and regulate gene expression, emergence of mutations, and tumor immune microenvironment[18]. A classic example of tumor metabolic reprogramming is the "Warburg effect", in which cancer cells use glycolysis to replace normal cells that depend on aerobic metabolism for survival[19]. Abnormalities in glucose and lipid metabolisms in tumors have been the focus of recent studies[20]. To date, genes associated with lipid metabolism have not been fully explored and their functions in the pathogenesis, diagnosis, and treatment of HCC remain to be determined. In this study, we used multi-dimensional bioinformatic methods to screen abnormally regulated genes associated with lipid metabolism in HCC. These genes were then used to construct a prognostic prediction signature.

Dysregulation of genes associated with lipid metabolism has been implicated in HCC tumorigenesis. In particular, alcohol dehydrogenase 1A triggers oncogenic transformation of hepatocytes, leading to poor survival[21], whereas extracellular pigment epithelium-derived factor inhibits angiogenesis in HCC by inducing lipid metabolic disorders[22]. These insights into the molecular mechanisms and gene markers involved in the pathogenesis of HCC have enhanced our understanding of its metabolic profile. However, achieving clinical benefits from single-gene targets in HCC is challenging. In this study, we determined the relationships between lipid metabolism-related genes and clinical features of HCC. A prognostic signature (6-IS) with good predictive results was constructed. This prognostic signature was also associated with overall survival, clinical features, and metabolic signaling pathways in patients with HCC. The 6-IS comprised six genes (*FMO3*, *SLC11A1*, *RNF10*, *KCNH2*, *ME1*, and *ZIC2*) obtained using multidimensional algorithms. This signature was shown to overcome single-gene shortcomings, such as interference from other factors. We found that FMO3 suppresses tumor progression by decreasing cellular viability; therefore, it is a protective index. This finding was in concordance with a previous study[23]. It was also revealed that ME1 or ZIC2, which exhibit stem-cell features, were correlated with poor prognosis, and therefore, risk indices[24,25]. It has been reported the presence of potential errors and biases in their analyses. For this reason, a statistical signature with multiple genes comprising clinical information to improve the efficiency of prognostic prediction was constructed. In terms of prognostic prediction, the 6-IS performed better than other models from external datasets. Further studies are needed to validate the performance of 6-IS in a prospective cohort.

Immune estimation tools, such as TIMER and ESTIMATE, were used to calculate immune scores to assess the immune infiltration of cells across groups. We found that HCC was characterized by heavy infiltration of immune cells, and that the inflammatory responses in the liver are the main mechanisms contributing to hepatitis, cirrhosis, and HCC. This finding was in concordance with previous findings[26]. Unlike studies that used the global transcriptome of HCC to analyze immune cell composition and perform molecular classification, we only used IMRGs to determine immune scores and perform metabolic stratification. A strong link between metabolism and immunity has been demonstrated during tumorigenesis[27]. Our study revealed that IMRGs associated with the regulation of immune cells during the pathogenesis of HCC. Metabolic and epigenetic pathways are important in regulating tumor immunity. Most epigenetic reprogramming genes are associated with fatty acid, cholesterol esters, and phosphatidylcholine metabolisms[28]. KEGG and GO analyses showed that the IMRGs differentially expressed between clusters were enriched in diverse metabolic pathways. Moreover, GSEA analysis revealed that upregulated or downregulated IMRGs used to construct 6-IS were associated with metabolic pathways. We hypothesized that the IMRGs were involved in several metabolic pathways that modulate the functions and phenotypes of immune cells during the pathogenesis of HCC.

Clinical features, such as AFP, TNM, tumor stage and grade, and other pathological classifications are considered in the clinical management of HCC[29]. However, these data are biased and lack specificity. There is a need to identify accurate indicators and phenotypes to improve existing diagnostic and therapeutic guidelines[30]. In this study, the OS was predicted based on AFP, stage, and TNM indicators. The performance of 6-IS was then compared with the above clinical features. The results showed that compared to other clinical features, 6-IS was superior in predicting HCC prognosis. In addition, 6-IS was also found to be an independent prognostic factor. Given that

6-IS is yet to be verified in prospective cohort studies, we suggest that it can be combined with traditional clinical features to improve the clinical management of HCC.

Conclusions

Summarily, we present an IMRG-based signature to classify patients with HCC into molecular clusters based on metabolic profiles. The 6-IS was found to be a robust prognostic prediction marker for HCC. This signature was associated with clinical features, immune cells, and various functions. This study provides novel insights into the prognostic value of lipid metabolism in HCC.

Conflict of Interest

The Authors declare that they have no conflict of interests.

Acknowledgements

The research was supported by Shenzhen Science and Technology Innovation Commission (JCYJ20170307153704628); Health Scientific Research Project of Pingshan District, Shenzhen City (201714).

References

1) Siegel RL, Miller KD, Jemal A. Cancer statistics, 2018. CA Cancer J Clin 2018; 68: 7-30.
2) Cabibbo G, Craxì A. Epidemiology, risk factors and surveillance of hepatocellular carcinoma. Eur Rev Med Pharmacol Sci 2010; 14: 352-355.
3) Liu ZY, Lin Y, Zhang JY, Zhang YM, Li YQ, Liu ZH, Li Q, Luo M, Liang R, Ye JZ. Molecular targeted and immune checkpoint therapy for advanced hepatocellular carcinoma. J Exp Clin Cancer Res 2019; 38: 447.
4) Rui L. Energy metabolism in the liver. Compr Physiol 2014; 4: 177-197.
5) Hu B, Lin JZ, Yang XB, Sang XT. Aberrant lipid metabolism in hepatocellular carcinoma cells as well as immune microenvironment: A review. Cell Prolif 2020: e12772.
6) Nakagawa H, Hayata Y, Kawamura S, Yamada T, Fujiwara N, Koike K. Lipid metabolic reprogramming in hepatocellular carcinoma. Cancers 2018; 10: 447.
7) Wu JM, Skill NJ, Maluccio MA. Evidence of aberrant lipid metabolism in hepatitis C and hepatocellular carcinoma. HPB 2010; 12: 625-636.
8) Currie E, Schulze A, Zechner R, Walther TC, Farese RV, Jr. Cellular fatty acid metabolism and cancer. Cell Metab 2013; 18: 153-161.
9) Beyoglu D, Imbeaud S, Maurhofer O, Bioulac-Sage P, Zucman-Rossi J, Dufour JF, Jeffrey RI. Tissue metabolomics of hepatocellular carcinoma: tumor energy metabolism and the role of transcriptomic classification. Hepatology 2013; 58: 229-238.
10) Che L, Pilo MG, Cigliano A, Latte G, Simile MM, Ribback S, Frank D, Matthias E, Chen X, Diego FC. Oncogene dependent requirement of fatty acid synthase in hepatocellular carcinoma. Cell cycle 2017; 16: 499-507.
11) Bidkhori G, Benfeitas R, Klevstig M, Zhang C, Nielsen J, Uhlen M, Jan B, Adil M. Metabolic network-based stratification of hepatocellular carcinoma reveals three distinct tumor subtypes. Proc Natl Acad Sci U S A 2018; 115: E11874-E11883.
12) Brunet JP, Tamayo P, Golub TR, Mesirov JP. Metagenes and molecular pattern discovery using matrix factorization. Proc Natl Acad Sci U S A 2004; 101: 4164-4169.
13) Gui J, Li H. Penalized Cox regression analysis in the high-dimensional and low-sample size settings, with applications to microarray gene expression data. Bioinformatics 2005; 21: 3001-3008.
14) Liu GM, Zeng HD, Zhang CY, Xu JW. Identification of a six-gene signature predicting overall survival for hepatocellular carcinoma. Cancer Cell Int 2019; 19: 138.
15) Qiao GJ, Chen L, Wu JC, Li ZR. Identification of an eight-gene signature for survival prediction for patients with hepatocellular carcinoma based on integrated bioinformatics analysis. PeerJ 2019; 7: e6548.
16) Wang Z, Teng D, Li Y, Hu Z, Liu L, Zheng H. A six-gene-based prognostic signature for hepatocellular carcinoma overall survival prediction. Life Sci 2018; 203: 83-91.
17) Zheng Y, Liu Y, Zhao S, Zheng Z, Shen C, An L, Yuan YL. Large-scale analysis reveals a novel risk score to predict overall survival in hepatocellular carcinoma. Cancer Manag Res 2018; 10: 6079-6096.
18) Wang J-J, Lei K-F, Han F. Tumor microenvironment: recent advances in various cancer treatments. Eur Rev Med Pharmacol Sci 2018; 22: 3855-3864.
19) Yoshida GJ. Metabolic reprogramming: the emerging concept and associated therapeutic strategies. J Exp Clin Cancer Res 2015; 34: 111.
20) Buechler C, Aslanidis C. Role of lipids in pathophysiology, diagnosis and therapy of hepatocellular carcinoma. Biochim Biophys Acta Mol Cell Biol Lipids 2020; 1865: 158658.
21) Zahid KR, Yao S, Khan ARR, Raza U, Gou D. mTOR/HDAC1 crosstalk mediated suppression of ADH1A and ALDH2 links alcohol metabolism to hepatocellular carcinoma onset and progression in silico. Front Oncol 2019; 9: 1000.
22) Li C, Huang Z, Zhu L, Yu X, Gao T, Feng J, Hong HH, Yin HF, Zhou T, Qi WW, Yang ZH, Liu C,

Yang X, Gao GQ. The contrary intracellular and extracellular functions of PEDF in HCC development. Cell Death Dis 2019; 10: 742.

23) Hlady RA, Sathyanarayan A, Thompson JJ, Zhou D, Wu Q, Pham K, Lee JH, Chen L, Keith DR. Integrating the epigenome to identify drivers of hepatocellular carcinoma. Hepatology 2019; 69: 639-652.

24) Mihara Y, Akiba J, Ogasawara S, Kondo R, Fukushima H, Itadani H, Obara H, Kakuma T, Kusano H, Naito Y, Okuda K, Nakashima O, Yano H. Malic enzyme 1 is a potential marker of combined hepatocellular cholangiocarcinoma, subtype with stem-cell features, intermediate-cell type. Hepatol Res 2019; 49: 1066-1075.

25) Zhu P, Wang Y, He L, Huang G, Du Y, Zhang G, Yan XL, Xia PY, Ye BQ, Wang S, Hao L, Wu JY, Fan ZS. ZIC2-dependent OCT4 activation drives self-renewal of human liver cancer stem cells. J Clin Invest 2015; 125: 3795-3808.

26) Kurebayashi Y, Ojima H, Tsujikawa H, Kubota N, Maehara J, Abe Y, Minoru K, Masahiro S, Yuko K, Michiie S. Landscape of immune microenvironment in hepatocellular carcinoma and its additional impact on histological and molecular classification. Hepatology 2018; 68: 1025-1041.

27) Zhang Q, Lou Y, Bai XL, Liang TB. Immunometabolism: a novel perspective of liver cancer microenvironment and its influence on tumor progression. World J Gastroenterol 2018; 24: 3500-3512.

28) O'Neill LA, Kishton RJ, Rathmell J. A guide to immunometabolism for immunologists. Nat Rev Immunol 2016; 16: 553-565.

29) Juarez-Hernandez E, Motola-Kuba D, Chavez-Tapia NC, Uribe M, Barbero Becerra V. Biomarkers in hepatocellular carcinoma: an overview. Expert Rev Gastroenterol Hepatol 2017; 11: 549-558.

30) De Stefano F, Chacon E, Turcios L, Marti F, Gedaly R. Novel biomarkers in hepatocellular carcinoma. Dig Liver Dis 2018; 50: 1115-1123.